2015 IEEE 18th International Conference on Intelligent Transportation Systems

Driver-Activity Recognition in the Context of Conditionally Autonomous Driving

Christian Braunagel, Wolfgang Stolzmann
Daimler AG
Stuttgart, Germany
Email: {christian.braunagel,wolfgang.stolzmann}@daimler.com

Enkelejda Kasneci, Wolfgang Rosenstiel
University of Tübingen
Tübingen, Germany
{enkelejda.kasneci,wolfgang.rosenstiel}@uni-tuebingen.de

***Abstract*—This paper presents a novel approach to automated recognition of the driver's activity, which is a crucial factor for determining the take-over readiness in conditionally autonomous driving scenarios. Therefore, an architecture based on head- and eye-tracking data is introduced in this study and several features are analyzed. The proposed approach is evaluated on data recorded during a driving simulator study with 73 subjects performing different secondary tasks while driving in an autonomous setting. The proposed architecture shows promising results towards in-vehicle driver-activity recognition. Furthermore, a significant improvement in the classification performance is demonstrated due to the consideration of novel features derived especially for the autonomous driving context.**

I. Introduction

Detecting the task currently being performed by a driver is crucial for many different applications in the realm of intelligent vehicles, including the case of autonomous driving. The typical application field of automated driver-activity recognition is the detection of driving risks, e.g. when the driver is inattentive [1]. Recent developments in the field of autonomous driving give rise to new challenges, and therefore to new applications for driver-activity recognition. The classification of the driver's take-over readiness is one of these challenges. While driving conditionally autonomously, the vehicle takes over for a specific interval [2]. Thus, the driver hands over the full responsibility to the vehicle and its autonomous driving function and is then able to deal with secondary tasks or to relax in the vehicle. However, situations will occur in which the system for autonomous driving will reach its limits. Hence, it will not be possible to control the vehicle safely anymore. Typical examples would be the loss of the lane markings or reaching the end of the proper road. In such situations, the vehicle needs to perform a take-over request to hand over the control and, consequently, the responsibility to the driver. To perform the process of a take-over, the vehicle and driver have only a limited amount of time. In such situations a new question emerges: is the driver able to take over at that specific moment?

Many different factors such as the traffic scenario or the current weather conditions need to be considered to answer this question. Another crucial factor for determining take-over readiness is the driver's level of inattention, which is influenced by the secondary task being performed by the driver. Possible secondary tasks associated with autonomous driving [3], [4] show varying complexity dependent on the respective type of distraction e.g. auditory, visual, manual, or a combination thereof. It is assumed that, based on the increasing risk of near and actual crashes in non-autonomous driving situations when performing secondary tasks [5], that take-over quality degrades when performing secondary tasks, especially for tasks with increased complexity.

If it were possible to automatically detect secondary tasks while they are being performed, the driver's inattention level could be inferred. Consequently, the driver could be supported in the best possible manner during take-over situations. Current frameworks for driver-activity recognition commonly focus on body gestures and gaze direction estimations to identify the region where the driver's current interactions are taking place. In this paper, however, we will examine the employment of an architecture for driver-activity recognition in the context of conditionally autonomous driving based on eye- and head-movement patterns without relying on the error-prone gaze direction estimation.

II. Previous Work

Detection of the driver's current secondary task is one of the various applications of human activity recognition, e.g. in smart security surveillance, health monitoring, efficient human-machine interfaces, etc. Also, human activity recognition is at the focus of research in the field of computer vision [6]. Furthermore, there are some studies regarding the application of in-vehicle camera systems for the recognition of different types of activities inside the vehicle e.g. activities near the steering wheel area. Typically, the motion patterns of different body parts, e.g. motion of the hands, legs, the torso and the head, as well as the posture of the body are taken into account to infer driver activity. The detected activity does not have to be a concrete specified interaction with the vehicle or its surroundings, such as shifting into another gear, but it can describe an area-of-interest (AOI) the driver is currently paying attention to. These AOIs summarize all activities performed in the specified region. In this way, in [7] the driver tasks were related to three AOIs, namely wheel region interaction, gear region activity, and activity in the instrument cluster region. To distinguish reliably between the mentioned AOIs, the authors combined hand activity recognition [8] with the estimated gaze direction. Another more general approach for using semantic driver activity analysis that could easily be extended on multiple sensor types was introduced in [9].

In addition to the detection of body-part motions, posture, and gaze direction based on computer vision methods, wearable sensors can provide additional and highly accurate data [10]. To detect distracted driving behavior, wearable sensors for the driver's legs and head were used in [11]. It was noted

978-1-4673-6596-3/15 $31.00 © 2015 IEEE
DOI 10.1109/ITSC.2015.268

that the distracted activity of using a mobile phone can be detected reliably with the intrusive head sensor. Eye movement analysis measured by intrusive sensor systems, such as electrooculography (EOG) or head-mounted eye trackers, has been the target of growing interest in the field of human activity recognition in the last years. Eye movements were first considered as a possible information source for activity recognition by Bulling et al. [12]. To classify different office activities, such as browsing the web or reading a text, [12] recorded the eye movements by means of EOG, detected basic eye patterns, namely saccades, fixations and blinks, and extracted multiple features based on these patterns. The authors reported that eye movement analysis is suitable for activity recognition. Based on these findings, Banerjee et al. [13] analyzed time, frequency, and time-frequency correlated eye signal features to recognize eight different tasks. These features showed promising results in light of the high measurement frequency of 250Hz. Besides the above work based on EOG, the increasing signal quality of eye-tracking systems facilitates eye movements recording. Head-mounted eye trackers enabled a new approach combining eye movement analysis and visual features due to the available eye and field camera [14]. Using the Google Glass platform as a sensor to measure eye blinks and head motion patterns, it was verified in [15] that these standard sensors in combination with just four features yield the potential for human activity recognition. Besides the typical visual-based tasks, such as watching a movie and reading, the analyzed activities in [15] also contained a demanding cognitive activity, namely solving mathematical problems, and a physical activity, namely sawing. According to [15], the cognitive task was hard to classify due to its dual character: writing the answer and looking at the assignment sheet.

Our main contribution is twofold. To the best of the author's knowledge, this is the first work on the recognition of specific driver activities in the context of conditionally autonomous driving that goes beyond the detection of AOIs the driver is currently interacting with. Furthermore, we provide a thorough examination and evaluation of several features derived from eye- and head-tracking signals with respect to their applicability on automated secondary task recognition.

III. Proposed Approach

The basis for this approach to detect the driver's activities is built on a previously introduced framework [16] and shown in Fig.1. This architecture can be divided into two paths which are merged at the classification step: one path for eye-tracking, which is derived of the framework introduced in [12], and a novel path for head-tracking. The following will describe modifications of the original eye-tracking path as well as the novel head-tracking path. Furthermore, different varieties for the feature extraction steps will be outlined for a later comparison.

A. Architecture for activity recognition

Starting with the eye-tracking path, shaded in light gray in Fig.1, mobile or in-vehicle eye tracking systems are used to record the eye movements instead of an EOG system as in [12]. Due to the often significant lower frequency and the typical challenges concerning video-based eye trackers, e.g. changing

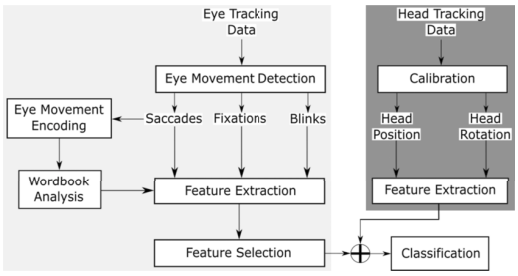

Fig. 1. Overview of the applied architecture.

illumination conditions, individual shape of the pupil, etc., a lower signal quality has to be expected. A Bayesian online mixture model as described in [17] was applied to distinguish between saccades and fixations. The algorithm provides a considerable advantage for detecting the eye movements in different situations. Due to the permanent online adaption of the two Gaussian distributions of the mixture model, the algorithm is able to adapt to the highly intra- and inter-individual eye patterns. In the case of a camera signal, eye blinks are usually not explicitly detected but modeled from the data [18]. The actual blink detection in this work consists of two steps. In the first step, signal parts with a low signal quality are deleted. Therefore, a moving window of size $5\,\mathrm{sec}$ is shifted over the whole signal while calculating the amount of invalid values. If the percentage of invalid data is greater than 30%, this signal portion will not be considered for the next analysis step. The idea behind this is to reduce the amount of false detections in areas where the signal quality is inacceptable. In a second step, all remaining sequences in which the eye tracker was not able to detect the pupil, will be labelled as an eye blink of a certain duration t if the following threshold criteria are fulfilled:

$$|th_{min} - tol| \leq t \leq |th_{max} - tol|. \tag{1}$$

The threshold values from (1) were chosen to $th_{min} = 0.1\,\mathrm{sec}$ and $th_{max} = 0.4\,\mathrm{sec}$ according to [19] and represent the average minimum and maximum duration of an eye blink. The tolerance variable results from the circumstance that the duration of the examined events of invalid values typically does not correspond with the average eye blink duration. The reason is that the eye-tracking system is still able to detect the pupil while the eyelid is already moving downwards in the closing phase or moving upwards in the opening phase and the pupil is still visible. Therefore, the tolerance value has to be chosen according to the sampling rate f of the eye tracker and is set to $tol = \frac{1}{f}$.

The combined eye movement encoding and wordbook analysis perform a mapping of every saccade to a character depending on the amplitude and direction of the saccade. With the use of a moving window of a specified size l, which is shifted over the sequence of characters, all existing combinations of characters, called words, are detected and saved in the wordbook Wb_l as in [12]. After generating various features (see Section III-B), a feature selection by means of the FCBF (Fast Correlation-Based Filter) algorithm [20] is applied. FCBF chooses a subset of features according to the redundancy and relevance analysis based on the measure of correlation *symmetrical uncertainty*,

given by

$$SU(X,Y) = 2\left(\frac{IG(X|Y)}{H(X)+H(Y)}\right) \quad (2)$$

where IG is called information gain referred to the pair of features (X,Y) and H is the entropy. This method comes with the benefit of not being forced to choose the size of the subset a priori. Instead, a relevance threshold γ can be defined to decide if the correlation of any feature and a class C is high enough. For this study, γ was set to $\gamma = 0.1$.

The head-tracking path, shaded in dark gray in Fig.1, is based on the measured head position and head rotation. The calibration step is used to determine the driver's head orientation when looking straight ahead at the road. This is necessary for the later calculation of the head features and for the comparability among different test subjects. As for the eye-tracking path, the feature extraction step will be skipped here and explained in detail in Section III-B.

Finally, the selected eye and head features are merged and used for the training and testing of the classification model. A Support Vector Machine (SVM) was employed as classifier, since this type of classifier tends to be robust with regard to the overfitting difficulty due to the use of the regularization principle [21]. Furthermore, a Radial Basis Function (RBF) kernel is applied, because of earlier promising classification results of the combination SVM and RBF kernel [12], [13].

B. Feature Extraction

The two feature extraction steps of the head- and eye-tracking paths in Fig.1 are the heart of the later analysis. This work compares two variations of the feature extraction step of the eye-tracking path with regard to their applicability to the automated secondary task detection. The first variation contains 92 eye-based features all taken from literature mentioned in Section II. More specifically, 90 features are selected as suggested by [12]. These features, containing mean, variance, rate, and maximum values, can be separated into four groups: 62 features related to saccades, 5 features derived from fixations, 3 features related to blinks, and 20 wordbook features. The two left eye features of this variation describe the x- and y-coordinate of the centroid of a blink frequency histogram with the actually blink frequency shown on the x-axis and the number of occurrences of the particular frequency shown on the y-axis. The blink frequency was calculated by a sliding window of specified window and step size [15].

These features were already successfully applied for human activity recognition in lab environments. However, a conditionally autonomous driving scenario can be seen as far more dynamic and distracting than a static lab environment. Thus, diverging behavior of the test subjects is expected. A typical viewing behavior during a secondary task in the context of autonomous driving are gazes away from the secondary tasks towards the road [22] before returning the gaze towards the secondary task. Reasons for this behavior could be other traffic participants attracting the attention of the driver or fading attention towards the secondary task. This work refers to such behavior as *control gaze behavior* and *control gazes* respectively. Fig.2 presents an example of such a viewing behavior, showing the saccades towards the road (upper-left cluster) and the saccades towards the secondary task (lower-right cluster), exemplarily performed at the area of the center

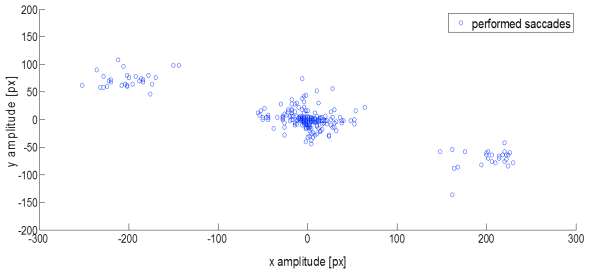

Fig. 2. Exemplary scatter plot of the control gaze behavior. Every point resembles a detected saccade with the horizontal/vertical amount of the amplitude on the x-/y-axis. The unit of the scales is pixel (px) dependent on the used camera system.

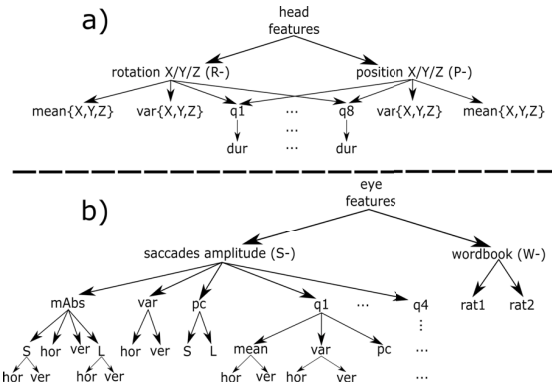

Fig. 3. Tree structure of the novel head and eye features introduced in this work. mAbs=mean of absolute values, var=variance, hor=horizontal, ver=vertical, S=small, L=large, pc=percentage, qX=quadrant number x, ratX=ratio of words of the size X, dur=duration, B=blink, cent=centroid.

console. Such behavior complicates the goal of detecting the driver activity, since the driver often interrupts the current secondary task, leading to eye and head movements that are not related to this task.

Therefore, this work examines novel eye and head features introduced to address the behavior of the test subjects in the vehicle. All these new introduced features are shown in the tree structure in Fig.3 with the appropriate notation as introduced by [12]. Every leaf node corresponds to an actual feature, while the parent nodes show the dependencies to the different head and eye patterns. Fig.3a) outlines 20 features derived from the head-tracking signal. The mean and variance features are calculated for every position and rotation in the 3D-space. To get an insight, where and for how long the driver's head was directed, the field of view is divided into eight quadrants as shown in Fig.4. The inner four quadrants result from the circumstance that the gaze and head direction straight ahead cannot be seen as an exact point but only as a narrow field of view. The size of the inner quadrants was set to $10°$ in x- and $5°$ in y-direction based on a previous analysis of the head direction. We introduce 32 novel eye-based features as listed in Fig.3b), where 20 of these features are based on the distribution of driver's saccades in the four outer quadrants $Q1$ to $Q4$ and the remaining 12 features can be seen as an addition to the above mentioned 92 features. However, in contrast to the features known from literature, we are using the absolute value of the amplitude, given by the notation *mAbs*, before

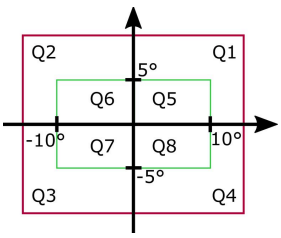

Fig. 4. Schematic segmentation of the driver's field of view in eight quadrants.

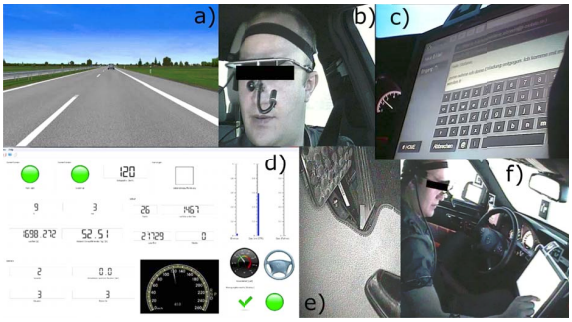

Fig. 5. Recorded video of the different camera perspectives and of the GUI for monitoring purpose.

calculating the mean value. Without using the absolute values, opposite saccade clusters as shown in Fig.2, would abrogate one another. The result would be a loss of information. The two wordbook features, namely *W-rat1* and *W-rat2*, pursue the idea to improve the classification of secondary tasks involving reading by calculating the ratio between the number of glances to the right and glances to the left. In the case of reading, this ratio should tend towards the glances to the right, since reading typically consist of many small glances in direction of reading. Therefore, all words mapped from saccades with any positive resp. negative horizontal amount of the amplitude are counted as glances to the right resp. left. This feature was calculated for the wordbook sizes $l = 1$ and $l = 2$. The remaining features, namely mean, variance, and percentage of the saccades contained in the different quadrants, reflect the distribution of the performed saccades among $Q1$ to $Q4$. Hence, these features try to determine if the clusters of the control gazes exist. The size of the inner quadrants was set to 75 px in x- and 25 px in y-direction based on a previous analysis of scatter plots similar to Fig.2.

IV. Results

A. Experiment

For evaluating the performance of the different combinations of the head and eye features, data was collected during a conditionally autonomous driving simulator study in the Mercedes-Benz Driving Simulator [23]. Here, the parts relevant to our issues are explained. The test subjects drove conditionally autonomously on a typical autobahn route for about 35 minutes at 120 km/h in a detailed driver's cabin of a Mercedes-Benz W212 E-Class. A touch screen was mounted in front of the center console so that the driver could perform the secondary tasks. The set of secondary tasks included, among other things; watching a movie, reading news, writing an email, and being idle. 85 test subjects participated in this study, divided into an experimental group of 74 test subjects performing secondary tasks and into a control group of 11 test subjects performing only the idle task. Introducing this second group of subjects allowed examining the driver's visual behavior in the context of automated driving, where the driver was not involved in a secondary task. The eye movements of the test subject were recorded by means of a mobile Dikablis eye tracker [24], measuring at a sampling rate of 25Hz. The head movements were recorded with a laserBIRD device [25], a precise optical head-mounted laser scanner, at a sampling rate of 50Hz. The eye and head tracking systems are shown in Fig.5 b) and f). Inside the cabin, four video cameras were mounted at different angles allowing the permanent observation of the driver's face, the footwell, the steering wheel area, and the touch screen (see Fig.5). During the experiment, an interface for monitoring purpose of various vehicle and route information was displayed and added to the recorded video data shown in Fig.5d). At the beginning of each experimental drive, a short calibration was performed. A marker was shown on the screen in front of the driver's cabin and the test subject was asked to focus the marker while keeping the head as straight as possible for about 5 sec. The recorded head position and rotation were used in the calibration step described in Section III.

B. Evaluation

For the evaluation, only data from 73 of the former 85 test subjects could be used due to missing signals of the head- and/or eye-tracking system for 12 test subjects of the experimental group. A One-Against-All Multi-Class SVM classification coupled with a leave-on-out cross-validation method was conducted, i.e. the model was trained with the data samples of 72 test subjects, tested with the samples of the left test subject and this procedure was repeated for every possible combination. This approach was chosen in order to provide as many training samples as possible to cover as much different driver behaviors as possible. Furthermore, this approach ensured that the evaluation was driver independend, i.e. the model never saw any data samples of the driver used for the testing phase. Since the number of performed secondary tasks varied among the test subjects and the required duration time of some tasks was driver dependent, e.g. because of the reading rate, the amount of data samples is not equal for the different tasks. Consequently, training the model with an unbalanced data set was prevented by only taking the same number of randomly chosen data samples, more precisely the minimum number of samples among all secondary tasks, of every task.

C. Experimental Results

The first step was to apply only the eye features that are known from related work in order to determine how these features perform in the context of autonomous driving. The features were calculated for non-overlapping sequences of a duration of 90 sec. On average one hour of recorded data per secondary task was used to train the model. Fig.6 shows the confusion matrix of the classification result. Obviously, the used features are still able to distinguish between the different visual tasks and the idle task in the simulated driving scenario.

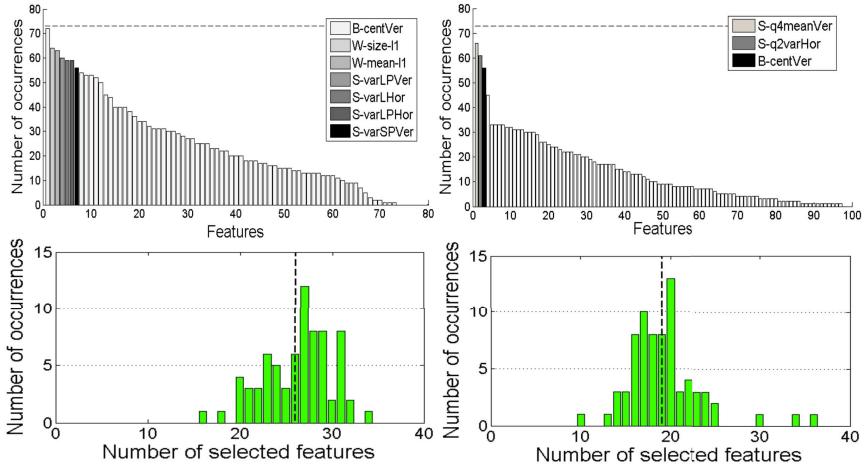

Fig. 8. Histograms of the selected features for the analysis of the eye features taken from the literature (left) and for the combination with the novel eye features (right). The upper histograms show the features arranged according to their number of selections by the FCBF algorithm. The features with the gray shaded bars were selected for more than 75% of the test subjects. The lower histograms show the total number of selected features over all test subjects.

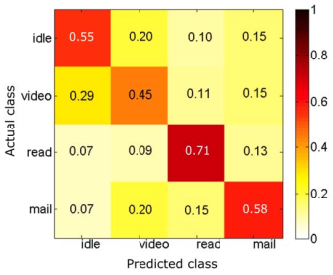

Fig. 6. Confusion matrix showing the classification results based on 92 features derived from the eye-tracking signal.

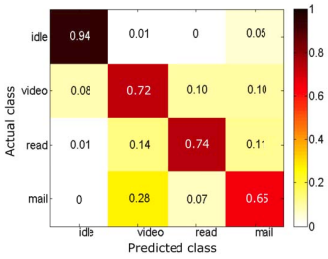

Fig. 7. Classification result using the combination of the 92 eye-based features from Fig.6 and 32 novel eye-based and 2 novel head features.

However, with a recall of 0.57% and a precision of 0.5%, the model performs significantly worse than in the known lab environments for which the above features were originally designed. The two histograms on the left part of Fig.8 show the features selected by the FCBF. In the upper histogram, we see the seven most selected features ordered by the number of selections shaded in gray. Each of these features was selected at least for 75% of the test subjects. The cumulative histogram below it shows the number of selected features. The average number of selected features among all 73 test subjects is marked with a dotted vertical line at 26 features.

To improve this classification result, the next step focused on improving the detection of the idle task based on the novel 20 head features as introduced in Section III-B. Three binary classification runs, namely idle task versus video, reading, or writing task, were performed, analyzing the potential of the head features to separate the idle task from the three other visual tasks. In all of the three cases, the two most relevant and most often selected features were *RP-q4dur* and *RP-q1dur*. The duration for which the head direction stays in one of the two outer quadrants on the right appears to be enough for a reliably classification. All the other features did not seem to be of any relevance. With respect to these findings, the same three classification runs were repeated using only the *RP-q4dur* and *RP-q1dur* feature. The recall of 0.93% and an average precision value of 0.9% over the three classification results confirmed the identification of two features which can discriminate the idle task from the remaining secondary tasks. The final analysis combined the novel eye features with the two a priori extracted head and the 92 eye features taken from literature. In comparison to the first confusion matrix, a significantly improved classification result was obtained as shown in Fig.7. Both recall and precision improved compared to the classification with just the 92 eye features by 20% to a recall of 0.76% and a precision of 0.7%. The best classification is reached by the idle task with a true positive value of 94% while the worst classification result of the mail task can be detected in 65% of cases. The difficulty in detecting the mail task lies in the dual character of the task: it combines segments where the driver is reading and, while writing and focusing on the keypad, segments with unstructured eye movements similar to the movie sequences. The high classification rate of the reading task was not further increased since the new features seem to hold no additional information to detect this task. Furthermore, the upper histogram of Fig.8 shows that for the combination of all eye features, a smaller set of features emerges used for more than 75% of the test subjects. The two best features for this analysis are *S-Q4meanVer* and *S-Q2varHor*, both extracted from the two quadrants directly related to the clusters of saccades emerging from the control gaze behavior of the driver. From the histogram below it

TABLE I. SUMMARY OF THE CLASSIFICATION RESULTS.

92 eye-based features				All features		
Task	**ACC**	**Precision**	**Recall**	**ACC**	**Precision**	**Recall**
idle		0.47	0.55		0.85	0.94
video		0.72	0.45		0.87	0.72
reading		0.6	0.71		0.72	0.74
mail		0.2	0.58		0.35	0.65
Ø	0.53	0.5	0.57	0.77	0.7	0.76

can be deduced that the total number of selected features per test subject decreases on average by 7 features to 19 features. Hence, these features seem to contain most relevant information, able of greatly improving the classification result even with a decreased number of features. As presented in Table I, the novel features resulted in a marked improvement of the mean classification accuracy (ACC) from 53% to 77%.

V. CONCLUSION

A novel approach to automated recognition of the driver's activity based on eye- and head-tracking data was presented. Despite a new framework, a set of novel eye- and head-based features for the automated classification of secondary task was introduced, especially designed for the context of autonomous driving. The architecture for secondary task recognition was evaluated on a large data set with 73 subjects derived from an extensive simulator study conducted at the Mercedes-Benz moving base simulator. The new features lead to a great improvement of the classification result, and thus to an increase in the classification accuracy from 0.53% to 0.77%. Eye features directly linked with the introduced control gaze behavior and two head features reflecting the head direction of the driver were of particular benefit. The high recall of the idle task, due to the head features, implies the distinction between an idle or a busy driver even with close-to-production driver monitoring systems of a first generation. Future work will involve applying the novel architecture to shorter sequences of the secondary tasks and examine the potential of the approach for additional tasks, such as tasks involving handheld devices.

REFERENCES

[1] Y. Dong, Z. Hu, K. Uchimura, and N. Murayama, "Driver inattention monitoring system for intelligent vehicles: A review," *IEEE Transactions on Intelligent Transportation Systems*, vol. 12, no. 2, pp. 596–614, 2011.

[2] S. International, *J3016: Taxonomy and Definitions for Terms Related to On-Road Motor Vehicle Automated Driving Systems*, SAE International Std., 2014.

[3] I. Petermann-Stock, L. Hackenberg, T. Muhr, and C. Mergl, "Wie lange braucht der Fahrer - Eine Analyse zu Übernahmezeiten aus verschiedenen Nebentätigkeiten während einer hochautomatisierten Staufahrt," *6. Tagung Fahrerassistenzsysteme. Der Weg zum automatischen Fahren*, 2013.

[4] R. E. Llaneras, J. Salinger, and C. A. Green, "Human factors issues associated with limited ability autonomous driving systems: Drivers' allocation of visual attention to the forward roadway," in *Proceedings of the seventh international driving symposium on human factors in driver assessment, training, and vehicle design, Bolton Landing, New York*, 2013, pp. 92–98.

[5] T. A. Dingus, S. Klauer, V. Neale, A. Petersen, S. Lee, J. Sudweeks, M. Perez, J. Hankey, D. Ramsey, S. Gupta *et al.*, "The 100-car naturalistic driving study, phase ii-results of the 100-car field experiment," NHTSA, Tech. Rep., 2006.

[6] P. Turaga, R. Chellappa, V. S. Subrahmanian, and O. Udrea, "Machine recognition of human activities: A survey," *IEEE Transactions on Circuits and Systems for Video Technology*, vol. 18, no. 11, pp. 1473–1488, 2008.

[7] E. Ohn-Bar, S. Martin, A. Tawari, and M. M. Trivedi, "Head, eye, and hand patterns for driver activity recognition," in *22nd International Conference on Pattern Recognition (ICPR), 2014*. IEEE, 2014, pp. 660–665.

[8] E. Ohn-Bar and M. M. Trivedi, "Beyond just keeping hands on the wheel: Towards visual interpretation of driver hand motion patterns," in *IEEE 17th International Conference on Intelligent Transportation Systems (ITSC), 2014*. IEEE, 2014, pp. 1245–1250.

[9] S. Park and M. Trivedi, "Driver activity analysis for intelligent vehicles: issues and development framework," in *Intelligent Vehicles Symposium, 2005. Proceedings. IEEE*. IEEE, 2005, pp. 644–649.

[10] O. D. Lara and M. A. Labrador, "A survey on human activity recognition using wearable sensors," *Communications Surveys & Tutorials, IEEE*, vol. 15, no. 3, pp. 1192–1209, 2013.

[11] A. Sathyanarayana, S. Nageswaren, H. Ghasemzadeh, R. Jafari, and J. H. Hansen, "Body sensor networks for driver distraction identification," in *IEEE International Conference on Vehicular Electronics and Safety, 2008. ICVES 2008.* IEEE, 2008, pp. 120–125.

[12] A. Bulling, J. A. Ward, H. Gellersen, and G. Troster, "Eye movement analysis for activity recognition using electrooculography," *IEEE Transactions on Pattern Analysis and Machine Intelligence*, vol. 33, no. 4, pp. 741–753, 2011.

[13] A. Banerjee, S. Datta, A. Konar, D. Tibarewala, and J. Ramadoss, "Cognitive activity recognition based on electrooculogram analysis," in *Advanced Computing, Networking and Informatics-Volume 1*. Springer, 2014, pp. 637–644.

[14] Y. Shiga, A. Dengel, T. Toyama, K. Kise, and Y. Utsumi, "Daily activity recognition combining gaze motion and visual features," in *Proceedings of the ACM International Joint Conference on Pervasive and Ubiquitous Computing: Adjunct Publication*. ACM, 2014, pp. 1103–1111.

[15] S. Ishimaru, K. Kunze, K. Kise, J. Weppner, A. Dengel, P. Lukowicz, and A. Bulling, "In the blink of an eye: combining head motion and eye blink frequency for activity recognition with google glass," in *Proceedings of the 5th Augmented Human International Conference*. ACM, 2014, p. 15.

[16] E. Kasneci, T. C. Kübler, C. Braunagel, W. Fuhl, W. Stolzmann, and W. Rosenstiel, "Exploiting the potential of eye movements analysis in the driving context," *15. Internationales Stuttgarter Symposium Automobil- und Motorentechnik*, 2015.

[17] E. Tafaj, G. Kasneci, W. Rosenstiel, and M. Bogdan, "Bayesian online clustering of eye movement data," in *Proceedings of the Symposium on Eye Tracking Research and Applications*. ACM, 2012, pp. 285–288.

[18] K. Holmqvist, M. Nyström, R. Andersson, R. Dewhurst, H. Jarodzka, and J. Van de Weijer, *Eye tracking: A comprehensive guide to methods and measures*. Oxford University Press, 2011.

[19] R. Milo, P. Jorgensen, U. Moran, G. Weber, and M. Springer, "BioNumbers - the database of key numbers in molecular and cell biology," *Nucleic acids research*, vol. 38, no. suppl 1, pp. D750–D753, 2010.

[20] L. Yu and H. Liu, "Efficient feature selection via analysis of relevance and redundancy," *The Journal of Machine Learning Research*, vol. 5, pp. 1205–1224, 2004.

[21] C. M. Bishop *et al.*, *Pattern recognition and machine learning*. Springer New York, 2006, vol. 4, no. 4.

[22] K. Zeeb, A. Buchner, and M. Schrauf, "What determines the take-over time? An integrated model approach of driver take-over after automated driving," *Accident Analysis & Prevention*, vol. 78, pp. 212–221, 2015.

[23] E. Zeeb, "Daimler's new full-scale, high-dynamic driving simulator–a technical overview," in *Conference Proc. Driving Simulator Conference Europe, Paris*, 2010.

[24] *Dikablis - Das Blickerfassungssystem. Benutzerhandbuch Dikablis Software*, Ergoneers GmbH, Manching, 09 2011.

[25] *laserBird - Installation and Operation Guide*, Ascension Technology Corporation, 04 2004.